CHAPTER IV

NUMERICAL SOLUTIONS TO THE NONLINEAR SCHRÖDINGER EQUATION

4.1   Introduction

In general, analytical solutions to the full Maxwell wave equation for a nonlinear optical system do not exist. Even numerical solutions to the wave equation are extremely difficult to implement due to the dimensionality of the problem. The vector form of the wave equation is a four-dimensional (three spatial, one temporal), second-order partial differential equation. Thus, approximations based on propagation conditions and experimental results are needed in order to solve an approximate scalar form of the wave equation, *i.e.* the nonlinear Schrödinger equation. However, the approximations listed in the previous chapter do limit the generality and validity of the solutions. For example, the condition extreme nonlinearity, as for the case in supercontinuum generation, is a propagation regime where slowly varying envelope approximation may be violated.

The purpose of this chapter is to provide an introduction to a very powerful method in numerically solving the NLSE, known as the split-step Fourier method (SSFM) [15]. The chapter will begin with a list pointing the advantages of the SSFM

compared to finite-difference methods. Then, the SSFM the symmetric SSFM will be introduced. The chapter will then detail the inclusion of the Raman effect in the numerical solution.

4.2   Why use the Split-Step Fourier Method?

The SSFM is the technique of choice for solving the NLSE due to its easy implementation and speed compared to other methods, notably time-domain finite-difference methods [73]. The finite difference method solves the Maxwell's wave equation explicitly in the time-domain under the assumption of the paraxial approximation. The SSFM falls under the category of pseudospectral methods, which typically are faster by an order of magnitude compared to finite difference methods [74]. The major difference between time-domain techniques and the SSFM is that the formal deals with all electromagnetic components without eliminating the carrier frequency. As shown in the previous chapter, the carrier frequency is dropped from the derivation of the NLSE. Thus, finite difference methods can account for forward and backward propagating waves, while the NLSE derived for the SSFM cannot. Since the carrier frequency is not dropped in the form of the electric field, finite-difference methods can accurately describe pulse propagation of nearly single-cycle pulses. While the finite difference method may be more accurate than the SSFM, it is only at the cost of more computation time.

In practice, the method chosen to solve the NLSE depends on the problem at hand. For pulse propagation for telecommunication applications (~100 ps pulses through

80 km of fiber with dispersion and SPM) the SSFM works extremely well and produces results that are in excellent agreement with the experiments [75, 76]. However, the SSFM would not work for modeling fiber Bragg gratings where there exists a forward and backward propagating wave. This thesis demonstrates that the SSFM also works efficiently and accurately for describing pulse propagation in microstructure fiber.

4.3   The Split-Step Fourier Method

The mathematical terms due dispersion and nonlinearity are separate and decoupled in the NLSE. It is this fact that allows the use of the SSFM for solving the NLSE. By looking at NLSE, the operators $\hat{D}$ and $\hat{N}$ can be written to correspond to the dispersive (and absorptive) and nonlinear terms respectively (ignoring the Raman effect),

$$\hat{D} = -\frac{\alpha}{2} - \sum_{m=2} \frac{i^{m-1}}{2^{m-1}} \beta_m \frac{\partial^m}{\partial t^m} \tag{4.1}$$

and

$$\hat{N} = i\gamma \left(|E(z,t)|^2 + \frac{2i}{\omega_0 E(z,t)} \frac{\partial}{\partial t} \left(|E(z,t)|^2 E(z,t) \right) \right) \tag{4.2}$$

where $E(z,t)$ is the complex field envelope at step z and time t. The NLSE then can be written in the operator form as

$$\frac{\partial E(z,t)}{\partial z} = (\hat{D} + \hat{N}) E(z,t). \tag{4.3}$$

136

where

$$E(jh,t) = \exp\left[h\left(\hat{D} + \hat{N}\right)\right]E((j-1)h,t), \qquad (4.4)$$

is a solution to the differential equation at step $z=jh$ (j is an integer). Note that the $\hat{N}$ operator multiplies the field solution *and* is a function of the solution $E(z,t)$. The $\hat{D}$ operator is a differential operator expressed in terms of time derivatives that operate on $E(z,t)$. To reduce the computational time, the operation of $\hat{D}$ is performed in the frequency domain; this transforms the derivatives in the time domain to a multiplication in the frequency domain. After taking the Fourier transform of $\hat{D}$ the multiplicative operator in the frequency domain is obtained,

$$\hat{D}(i\omega) \equiv \mathcal{F}\{\hat{D}\} = \mathcal{F}\left\{-\frac{\alpha}{2} - \sum_{m=2}\frac{i^{m-1}}{2^{m-1}}\beta_m\frac{\partial^m}{\partial t^m}\right\} = -\frac{\alpha}{2} - \sum_{m=2}\beta_m\frac{i^{m-1}}{2^{m-1}}(i\omega)^m.$$

$$(4.5)$$

The SSFM is an iterative process that determines the field solution for spatial steps of h. This is performed step-by-step for the entire length of the fiber. The procedure during one step is illustrated in Figure 4.1. A dielectric medium of length L is broken into $s_L=L/h$ steps of length h. The field propagation solution $E(jh,t)$ per spatial step h at the step jh ($j=1,2,\ldots s_L$) for the entire length of fiber using relation

$$E(jh,t) \approx \mathcal{F}^{-1}\left\{\exp\left(h\hat{D}(i\omega)\right)F\left\{\exp\left(h\hat{N}\right)E((j-1)h,t)\right\}\right\}, \qquad (4.6)$$

where $E((j-1)h,t)$ is the field solution from the previous step. The approximation

$$\exp\left[h(\hat{D}+\hat{N})\right] \approx \exp\left[h\hat{D}\right]\exp\left[h\hat{N}\right] \tag{4.7}$$

is used in rewriting Eq. (4.4) to Eq. (4.6). The operation of $\hat{N}$ occurs in the middle of the step and is the first operator to act on $E(jh,t)$. The effect of dispersion is determined in the frequency domain. The field solution is Fourier transformed, operated on by $\hat{D}$ and then back transformed to give the solution $E(jh,t)$ at step jh.
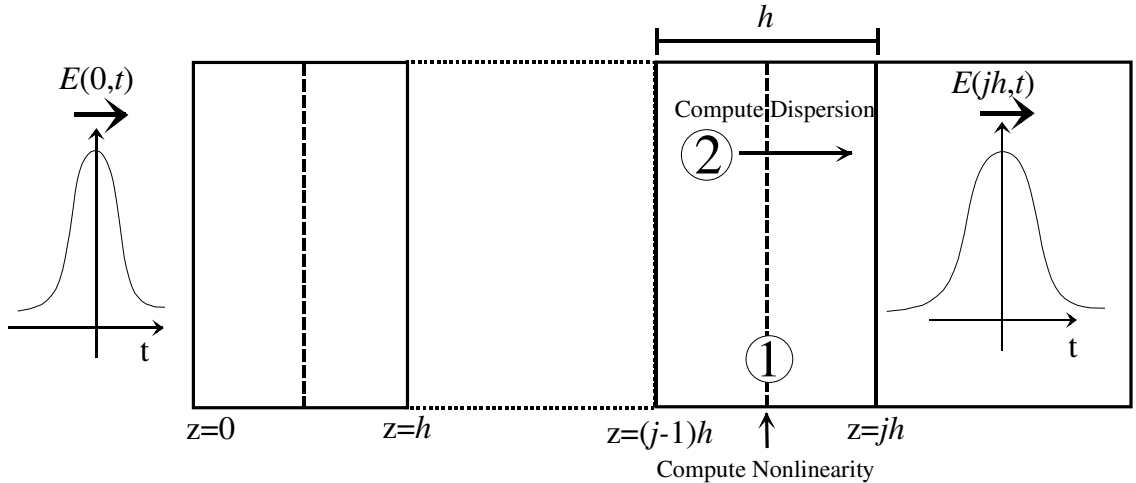

Figure 4.1   The SSFM for one iteration of step h starting at $z=(j-1)h$. The initial pulse $E(0,t)$ enters the medium of length L. The length is broken into $s_L=L/h$ steps of length h. The field solution at $z=jh$ is determined by:

138

1. Calculate the nonlineary at step midpoint : $\exp\left(h\hat{N}(i\omega)\right)E((j-1)h,t)$

2. Calculate the dispersion over step h in the frequency domain:

$$\exp\left(h\hat{D}(i\omega)\right)\mathcal{F}\left\{\exp\left(h\hat{N}(i\omega)\right)E((j-1)h,t)\right\}$$

Solution at $z = jh \Rightarrow E(jh,t) \approx \mathcal{F}^{-1}\left\{\exp\left(h\hat{D}(i\omega)\right)\mathcal{F}\left\{\exp\left(h\hat{N}(i\omega)\right)E((j-1)h,t)\right\}\right\}$

3. Repeat iterations till $z = s_L h = L$, where L is the length of the fiber,
   for the final solution $E(L,t)$.

Note that the form of field solution $E(z,t)$ is in general complex so it contains both intensity and phase information. The computation speed of the SSFM is due to 1) calculating the dispersion in the frequency domain thus avoiding any numerical derivatives, and 2) using the fast Fourier transform to go between the frequency and time domains.

4.4   Spectral/Temporal Sampling and Windowing

Great care must be taken in deciding the format, length, and temporal/spatial resolution of the complex array that numerically represents the quantity $E(z,t)$. Although the use of the FFT provides a robust method for computing the Fourier transform, it does impose restrictions on the sample array format. The sample array of $E(z,t)$ for each value of z must have $N=2^m$ points required by the FFT. Typically, the starting field $E(z=0,t)$ contains the intensity and phase of the input pulse. The initial array $E(0,t)$ must sample the initial pulse with adequate temporal resolution and be temporally wide enough to prevent aliasing and wrapping errors. The "adequate" sampling rate is given by the

Nyquist theorem, which states that the minimum sample frequency is twice the highest frequency sinusoidal component of significant amplitude [77]. For example, a Gaussian function $E(t)$ that has a intensity FWHM of Δt=100 fs (and a spectral width $\Delta \nu$=4.41 THz) an estimate of the highest significant frequency component would be at 4*$\Delta \nu$ or 17.7 THz. The function $I(t) \propto |E(t)|^2$ must be sampled at most by $\delta t = 1/(2*4*\Delta \nu)$ to meet the Nyquist Theorem. Typically, the sampling is performed by four times the Nyquist rate (ν_N=8$\Delta \nu$) or at δt=2.3 fs, which would have 15 points across the FWHM. Here, the pulse intensity spectral and temporal widths are represented in terms of the FWHM (Δt and $\Delta \nu$) since they are more related to measured quantities. Specifically, the Nyquist theorem apply to the widths of $E(t)$ and $E(\nu)$ since the FFT is used to obtain $E(\nu)$ from $E(t)$. However, by imposing the Nyquist theorem on $I(t)$, a stronger requirement on $E(t)$ is imposed since the temporal width of $E(t)$ is smaller than $I(t)$.

If the temporal resolution δt is chosen larger than that prescribed the Nyquist theorem, aliasing may occur in the frequency domain [56]. Here, frequency components beyond the Nyquist frequency are falsely translated (wrapped-around) into the spectral window. The aliased frequency components sum with the true frequency components, producing an incorrect spectrum. Aliasing is prevented by decreasing the size of δt, thus increasing the sampling rate.

The width of the temporal window ($N*\delta t$) must wide enough to accommodate any broadening due to dispersion for any z along the fiber length. Also, the spectral window

($N\delta v = 1/\delta t$) must be wide enough to accommodate any spectral broadening for any z along the fiber length due to the nonlinearity. If the solution $E(z,t)$ extends the window, errors will occur due to aliasing. Thus, beforehand there must be an estimate on what the final temporal width will be in order to choose the size of the temporal window (*i.e.* choosing N). The following table is a guide for choosing δt and N to accurately sample $E(t)$ for the SSFM.

Table 4.1 Determining the N sample points for the SSFM.
    On choosing N for using the SSFM for solving single pulse propagation, one must:

1) Determine the needed temporal resolution (δt) to accurately sample the initial pulse $E(0,t)$. A general rule for an accurate sample is to choose $\delta t = 1/(2*4*\Delta v)$ where Δv is the initial spectral FWHM. Or just use ~10 samples across the temporal FWHM.
2) Determine the total temporal window $N*\delta t$ that will be *at least* twice the final pulse temporal FWHM (Δt) at $z=L$.
3) Determine if the corresponding spectra resolution $\delta v = 1/N\delta t$ can accurately sample $E(0,v)$. Again, ~10 samples are desired across the spectral FWHM.
4) Determine if the corresponding spectral window $N*\delta v$ will be *at least* twice the final spectral FWHM (Δv) at $z=L$.
5) Determine if the choice of N will allow the solution to be performed in reasonable time.

Satisfying all the above constrains may be difficult, especially when modeling supercontinuum generation. In this case, a transform-limited pulse of 100 fs FWHM may broadened to a pulse that is >10 ps in length with a spectral width of ~900 nm. Setting the temporal and spectral windows for this case requires a very large N, since a proper δt and δv is needed to sample the initial pulse. This also would require a very large temporal and spectral window accommodate the large final Δt and δv.

4.5 Choosing the Spatial Step-Size

Unlike the restrictions on δt, there is no mathematical restriction on the step-size h for the SSFM. Keeping h very small would produce a very accurate at the cost of much computation time. Plus, choosing h smaller than the carrier wavelength λ_0 is physically meaningless, since the carrier frequency term in $\mathcal{E}(t)$ is dropped in the derivation of the NLSE. However, by choosing h to be too large the SSFM does not conserve spectral energy. The maximum choice of the step-size depends on the specific dispersive and nonlinear properties of the method: the dispersion length L_D and the nonlinear length L_N.

As defined in the prior chapter, the dispersion (Eq. 3.32) and the nonlinear lengths (Eq. 3.53) are characteristic length scales, which quantify the amount of dispersion and nonlinearity associated with propagation in a given fiber. Physically, L_D is the propagation length at which a Gaussian pulse broadens by a factor of $\sqrt{2}$ due to group-velocity dispersion. The term L_{NL} corresponds to the propagation length at which the SPM induced phase (φ_{NL}) is equal to 1 radian. In standard SMF (Corning SMF-128) at 1550 nm (P_0=1 W, Δt=1 ps, β_2= -20 ps^2/km), the corresponding values would be L_D=18 m and L_{NL}=50 m. The dispersion length for standard SMF illustrates the reason for using dispersion-shifted fiber (DSF), which has L_D=120 m, in any dispersion-managed OTDM link.

The dispersion and nonlinear lengths characterize the pulse propagation in a given fiber. GVD dominates the pulse propagation for fiber where $L \ll L_{NL}$ and $L \geq L_D$. Thus,

the operator $\hat{N}$ in the NLSE could be ignored and the NLSE could be solved analytically. Nonlinear effects (SPM) dominate the pulse propagation for fibers where $L \ll L_D$ and $L \geq L_{NL}$. Here, $\hat{D}$ the term could be ignored leading to an analytic solution to the NLSE.

Knowing the nonlinear and dispersion lengths associated with a given system allows for an educated choice on the step-size h to be made. The step-size should be considerably smaller than both L_D and L_{NL} for the solution via the SSFM to be meaningful. If the step-size is comparable to either L_D or L_{NL}, then the SSFM will not conserve energy. It can be determined if a chosen step-size is sufficient by computing the area under the finial and initial spectrum, hence computing the final and initial spectral energy Table 4.2 below is a prescription for determining the step-size for the SSFM:

Table 4.2   Determining the step-size h for the SSFM:
1) Compute L_D and L_{NL}. Compare L_D and L_{NL} to the fiber length L.
2) If $L \ll L_{NL}$ and $L \geq L_D$ or $L \ll L_D$ and $L \geq L_{NL}$, the NLSE can be solved analytically.
3) Choose a value for h such that $\lambda_0 < h < L_D$ and $\lambda_0 < h < L_{NL}$. If L is comparable to either L_D or L_{NL}, you may wish to make h small. Also, make this choice keeping computation time in mind.
4) Compute the solution via the SSFM. Compute the spectral energy before and after propagation. If these values are not approximately equal, decrease the size of h. If the finial and initial energies are nearly equal, enlarging h till a desired amount of error is reached can decrease the computation time.

Some variation of the SSFM computes the spectra energy per step and adapts the value of h to produce a desired energy error. Adapting the step-size is typically done for propagation through very long lengths of fiber to reduce the computation time.

Comparing the initial and final spectral energy is not a good metric for choosing the step-size when modeling the Raman effect. Optical energy is not conserved in SRS because photons are preferentially emitted at a lower frequency [66]. However, the classical photon number is conserved during the process of SRS. The step-size can be chosen here to conserve photon number.

4.6   Errors Associated with the Split Step Fourier Method

As seen above, the choice of the step-size and the temporal/spectral windows depend on the Nyquist Theorem, specific pulse propagation conditions and the amount of tolerable error. For a wrong choice of spectral/temporal windows, errors arise from aliasing. Also, for a wrong choice of spatial step-size, energy is not conserved by the SSFM. These errors can be avoided by the proper choice of step-size and spectral/temporal window. However, the primary source of error for the SSFM is due to the fact that the operators $\hat{D}$ and $\hat{N}$ do not commute (*i.e.* $\left[\hat{D}, \hat{N}\right] \neq 0$.). Physically, this implies that the origin of dispersive and nonlinear effects is intrinsically coupled. If the operators $\hat{D}$ and $\hat{N}$ do not commute, the approximation of Eq. (4.7) will provide an accurate solution to second-order in the step-size *h*.

For two operators, the expansion of the exponential in Eq. (4.4) can be obtained using the Baker-Hausdorff theorem [78],

$$\exp\left(h\hat{D}\right)\exp\left(h\hat{N}\right) = \exp\left\{h\left(\hat{D} + \hat{N} + \frac{1}{2}\left[\hat{D}, \hat{N}\right] + \frac{1}{12}\left[\hat{D} - \hat{N},\left[\hat{D}, \hat{N}\right]\right] + ...\right)\right\}.$$

(4.8)

Ignoring terms in the above expansion will add errors to the solution. The inclusion of more terms will be more difficult to implement and adds computation time. However, for problems that involve large dispersion, high effective nonlinearity or for short pulse widths (< 1 ps FWHM), the approximation given by Eq. (4.7) is not sufficient.

Another error encountered in the Eq. (4.7) is ignoring the change of γ as a function of length. Typically, this is not a source of error for modeling SMF; however, this could be a problem when trying to model dispersion decreasing fiber (DDF). This fiber is manufactured by reducing the core diameter along its length, usually the diameter changes with length exponentially [79]. The change in the core diameter alters the fiber's dispersion along its length. The $\hat{N}$ operator will have a dependence on z since the effective nonlinearity is inversely proportional to the mode effective. The error caused by this for modeling DDF is small and typically is ignored [80].

Also as discussed above, other avoidable errors can occur due to not choosing the correct temporal window and resolution. The origin of these errors is either due to aliasing or poor spectral/temporal resolution. These errors can always be avoided, by increasing the window size or data array size, but at the cost of more computation time and memory.

4.7   The Symmetrized SSFM

The error given by Eq. (4.7) can be further improved by the use of the symmetrized SSFM, which includes two terms of the expansion Eq. (4.8). The error now is due to the double commutator (third) term in the expression, which is of third order in step-size *h*. The solution at step *z=jh* can be determined by

$$E(jh,t) \approx \mathcal{F}^{-1}\left\{\exp\left(\frac{h}{2}\hat{D}(i\omega)\right)\mathcal{F}\left\{\exp\left(\int_{z}^{z+jh}\hat{N}(z')dz'\right)\mathcal{F}^{-1}\left\{\exp\left(\frac{h}{2}\hat{D}(i\omega)\right)\mathcal{F}\{E((j-1)h,t)\}\right\}\right\}\right\}$$

(4.9)

Note the significant differences between Eqs. (4.9) and (4.6). For the symmetrized SSFM, first the effect of dispersion over the length *h*/2 is computed, the effect of the nonlinearity occurs at the step midpoint, and finally the effect of dispersion is computed over *h*/2. The integral of the nonlinearity operator accounts for the change in γ over the step *h*, which in most cases can be treated as a constant. Note also that four FFTs are computed in the symmetrized SSFM compared to the two in the SSFM. The action per one step of the symmetrized SSFM is illustrated in Figure 4.1.
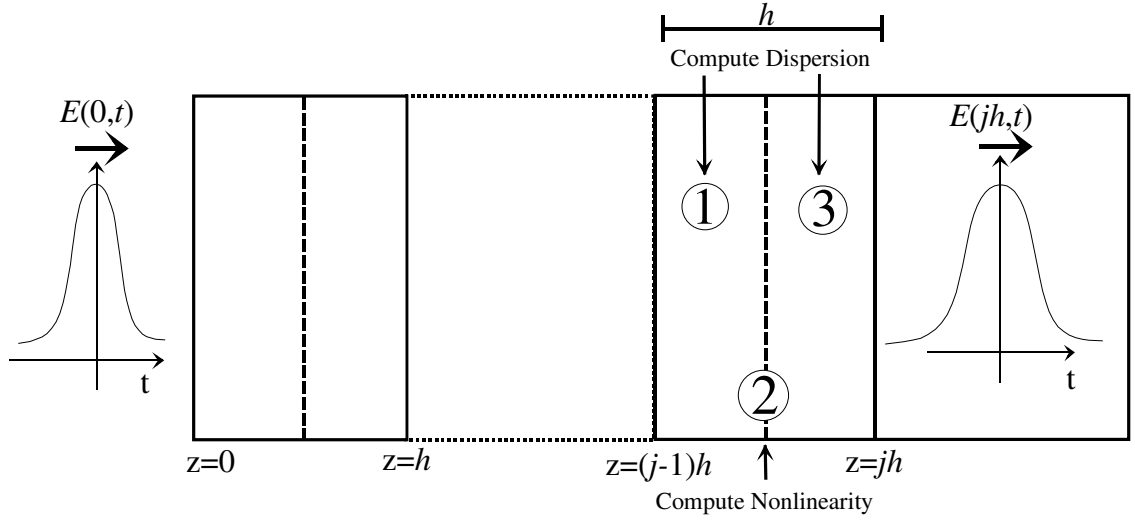
Figure 4.2   Schematic for one step of the symmetrized SSFM.   The field solution
$E(jh,t)$ is calculated from the solution $E((j-1)h,t)$ using the following steps:
1.Calculate the dispersion over step h in the frequency domain:

$$\exp\left(h\hat{D}(i\omega)\right)\mathcal{F}\{E((j-1)h,t)\}$$

2.Calculate the nonlineary at step midpoint :

$$\exp\left(h\hat{N}\right)\mathcal{F}^{-1}\left\{\exp\left(h\hat{D}(i\omega)\right)\mathcal{F}\{E((j-1)h,t)\}\right\}$$

Solution at $z = jh \Rightarrow \text{E}(jh,t) \approx \exp\left(h\hat{N}\right)\mathcal{F}^{-1}\left\{\exp\left(h\hat{D}(i\omega)\right)\mathcal{F}\{E((j-1)h,t)\}\right\}$

3. Repeat iterations till $z = s_L h = L$, where L is the length of the fiber,
        for the final solution $E(L,t)$.

4.8   Inclusion of Stimulated Raman Scattering in the Split-Step Fourier Method

The   inclusion   of   stimulated   Raman   scattering   into   the   SSFM   modifies   the

nonlinearity operator significant.   The nonlinear operator $\hat{N}$ can be written in a more

general form as

$$\hat{N} = \frac{i\gamma}{E(z,t)}\left(1+\frac{i}{\omega_0}\frac{\partial}{\partial t}\right)\left(E(z,t)\int_0^\infty R(t')\left|E(z,t-t')\right|^2 dt'\right), \qquad (4.10)$$

where $R(t)$ is the nonlinear time-response which includes electrical and vibrational (Raman) contributions to the third order susceptibility. The electronic contribution, responsible for the Kerr effect, will occur on a time scale much faster than the Raman contributions, which allows the time-response function to be written as [66]

$$R(t) = (1 - f_R)\delta(t) + f_R h_R(t) \tag{4.11}$$

where $\delta(t)$ is the delta function, f_R is the fractional contribution to the delayed Raman response $h_R(t)$. The electronic contributions of $R(t)$ comprise the SPM and self-steepening terms in the NLSE. The function $h_R(t)$ was discussed in Chapter III and plotted in Figure 3.8. It is obtained from the measured Raman gain spectrum $g_R(\omega)$ using Eq. 3.55. Note that the measured Raman gain is proportional to the imaginary portion of the complex third-order (Raman) susceptibility $\chi^{(3)}(\omega) = \chi^{(3)}\mathcal{F}\{h_R(t)\}$. The response $h_R(t)$ can be calculated by computing the real part of $\chi^{(3)}(\omega)$ via the Kramers-Kronig relationship [81] on measured Raman gain $g_R(\omega)$. Then. $h_R(t)$ is computed using the Fourier transform of the complex $\chi^{(3)}(\omega)$. Typically, $h_R(t)$ is determined directly from the imaginary part of (the Raman gain curve) and using the fact that $\mathrm{Re}\left[\chi^{(3)}(\omega)\right]$ is symmetric and $\mathrm{Im}\left[\chi^{(3)}(\omega)\right]$ is antisymmetric [82].

To include SRS properly in the SSFM, the Raman gain spectrum $g_R(\omega)$ or equivalently the Raman time response $h_R(t)$ the must be included into operator $\hat{N}$. This

can be performed in many ways. The least accurate manner is using the first order term

is a Taylor expansion of $\left|E(z,t-t')\right|^2$ in Eq. (4.10) and keeping the first order term

denoted T_R,

$$T_R = \int_0^\infty t' R(t') dt' \tag{4.12}$$

where for fused-silica $T_R \sim 3\text{-}5$ fs [3]. The time constant physically represents the initial

slope of the Raman gain spectrum [3]. The nonlinear operator then takes the form

$$\hat{N} = i\gamma\left(\left|E\right|^2 + \frac{2i}{\omega_0 E(z,t)}\frac{\partial}{\partial t}\left(\left|E\right|^2 E\right) - T_R\frac{\partial\left|E\right|^2}{\partial t}\right) \tag{4.13}$$

This is a very convenient form that just includes an extra numerical derivative with no

integration to be performed per step.

A second, more accurate method is to include the Raman time response $h_R(t)$,

which leads to a nonlinear operator of

$$\underbrace{\hat{N} = i\gamma(1-f_R)\left(\underbrace{\left|E\right|^2}_{\text{SPM}} + \underbrace{\frac{2i}{\omega_0 E}\frac{\partial}{\partial t}\left(\left|E\right|^2 E\right)}_{\text{Self-Steepening}}\right)}^{\text{Kerr Effect}}$$

$$+ i\gamma f_R\overbrace{\left(\left(\int_0^\infty h_R(t')\left|E(z,t-t')\right|^2 dt'\right) + \frac{2i}{\omega_0 E}\frac{\partial}{\partial t}\left(E\int_0^\infty h_R(t')\left|E(z,t-t')\right|^2 dt'\right)\right)}^{\text{Raman Effect}}. \tag{4.14}$$

The derivative of the integrated Raman time response is sometimes ignored. The function $h_R(t)$ is determined either from the measured Raman gain spectrum $g_R(\omega)$ [82] or by using the fitting function

$$h_R(t) = \frac{\tau_1^2 + \tau_2^2}{\tau_1 \tau_2^2}\sin(t/\tau_1)\exp(-t/\tau_2) \tag{4.15}$$

where τ_1=12.2 fs and τ_2=32 fs for fused-silica [66]. In regards to the SSFM, the inclusion of the integral in Eq. (4.14) requires a numerical integration to be performed over all values of t for each step $z=jh$. Inclusion of this integration dramatically increases the computation time. It is important to note that the Raman time response $h_R(t)$ is not measured directly, while the Raman gain $g_R(\omega)$ is measured directly. Thus, there may be many errors induced in the SSFM from the calculated $h_R(t)$.

The third method is to compute $h_R(t)$ from the measured Raman frequency response and use this instead of Eq. (4.15). Although, this is the most accurate it requires the Raman frequency response of a given fiber to be measured.

4.9   Four-Wave Mixing in the Split-Step Fourier Method

As discussed in Chapter III, a general four-wave mixing interaction can only happen when the phase matching criteria is met. The fiber net dispersion must be close to zero for $\Delta\beta=0$ and for efficient FWM to occur. Remember that SPM is a specific FWM term for which the phase matching criteria is automatically met, independent of the fiber dispersion and the pulse center wavelength. Excluding the effect of FWM is problematic when for fiber propagation at a center wavelength that is near the zero dispersion wavelength.   FWM *must* be considered for supercontinuum generation in microstructure fiber, which typically occurs for injected pulses centered at a wavelength near the zero GVD wavelength.

The Kerr term in the NLSE does contain the effect of FWM although the phase matching condition is not explicitly written in the NLSE. This is sufficient to include FWM into the SSFM. However, it has been noted [83] that SSFM may not correctly account for FWM since the action of the nonlinear and dispersion operator act independently. Also, since efficient FWM occurs under proper phase matching, which is a frequency domain equation, it may be better to treat FWM in the frequency domain. This comment is discussed in Section 4.11.2 when the total field formulation of François is introduced. As demonstrated later in the thesis, the modeling performed in this work describe accurately the presence of FWM in supercontinuum generation without resorting to a frequency domain representation of FWM.

4.10 SSFM Code Implementation

The code to implement the SSFM was written using both the programs *Mathematica*™ and *Matlab*™ (included in Appendix C at the end of the thesis). Initially, the SSFM was written in *Mathematica* for the spectral compression experiments, then rewritten in *Matlab*. This *Mathematica* program, which uses the symmetrized SSFM, was optimized for accuracy and not for speed. Later, the code was rewritten in *Matlab* for use with the supercontinuum generation experiments in microstructure fiber. These simulations demanded large array size to accommodate the wide temporal/spectral broadening due to propagation through the microstructure fiber. Plus, it was essential to incorporate SRS in the simulations, using either the linear approximation T_R or the Raman temporal response $h_R(t)$. The incorporation of SRS with a large array size was too time consuming to be implemented in *Mathematica*.

4.11 Other Methods for Solving the NLSE

This final section briefly discusses two other important methods for solving the NLSE. The first method is a technique method known as the inverse scattering method [73] and the second technique is a completely frequency domain technique known as the total field formulation [83]. Although these techniques are more rigorous and exact in solving the NLSE over the SSFM, both are very difficult to numerically implement, and the total field formulation requires significant computing capability.

4.11.1 The Inverse Scattering Method

The inverse scattering method was the first method to solve the NLSE for the specific case of soliton propagation by Zakharov and Shabat [13]. The method uses the initial field $E(z=0,t)$ to obtain the initial scattering data, then the propagation along z is found by solving the linear scattering problem. The final field $E(L,t)$ is reconstructed from the evolved scattering data. Typically, this method is used for soliton propagation [3]. The mathematical description of the inverse scattering method is very complex, the details can be found in Ref. [73]. However, for soliton propagation the inverse scattering method numerically reduces to an eigenvalue problem and a system of linear equations. The complexity of this method may force the SSFM to be desired, however, the inverse scattering method does not suffer from errors from separating the effects of fiber dispersion and nonlinearity. Plus, the inverse scattering method can be used to solve more generalized forms of the NLSE, like the Korteweg-de Vries equation [84, 85] or the Ginzberg-Landau equation.

The form of the NLSE for solitons to be solved by the inverse scattering method is

$$ i\frac{\partial U}{\partial \xi} = \mathrm{sgn}(\beta_2)\frac{1}{2}\frac{\partial^2 U}{\partial \tau^2} - \frac{L_D}{L_{NL}}|U|^2 U \tag{4.16} $$

where

$$ U = \frac{A(z,t)}{\sqrt{P_0}}, \quad \xi = \frac{z}{L_D}, \quad \text{and } \tau = \frac{t}{T_0}. \tag{4.17} $$

This is similar to the normalized NLSE derived in Chapter III. The above equation can be written to eliminate the soliton number L_D/L_{NL} by defining $u(\xi,\tau) = \left(L_D/L_{NL}\right)U(\xi,\tau)$. The equation Eq. (4.16) is integrable and can be expressed as two linear equations by Lax theory [84] as

$$L(\xi)u(\xi,\tau) = \zeta u(\xi,\tau) \tag{4.18}$$

and

$$\frac{\partial u(\xi,\tau)}{\partial\xi} = M(\xi)u(\xi,\tau), \tag{4.19}$$

where $L(\xi)$ and $M(\xi)$ are differential operators in τ. Equation (4.18) is an eigenvalue problem with eigenvalue ζ and Eq. (4.19) determines the ξ evolution of the wavefunction $u(\xi,\tau)$. The term $L(\xi)$ corresponds to the dispersion operator $\hat{D}$ since $L(\xi)$ evolves such that the spectrum remains constant. $L(\xi)$ and $M(\xi)$ are known as a Lax pair of the integrable system given by [13]

$$L(\xi) = \begin{bmatrix} i\dfrac{\partial}{\partial\tau} & u(\xi,\tau) \\ -u^*(\xi,\tau) & -i\dfrac{\partial}{\partial\tau} \end{bmatrix} \tag{4.20}$$

and

$$M(\xi) = \begin{bmatrix} i\dfrac{\partial^2}{\partial\tau^2} + \dfrac{i}{2}\left|u(\xi,\tau)\right|^2 & u(\xi,\tau)\dfrac{\partial^2}{\partial\tau^2} \\[2mm] -u^*(\xi,\tau)\dfrac{\partial^2}{\partial\tau^2} & -i\dfrac{\partial^2}{\partial\tau^2} - \dfrac{i}{2}\left|u(\xi,\tau)\right|^2 \end{bmatrix}. \tag{4.21}$$

The field $u(\xi{=}0,\tau)$ provides the initial scattering information $\Sigma(\xi{=}0)$ from the eigenvalue solution of Eq. (4.18). The evolution of the scattering data $\Sigma(\xi)$ is determined from the Eq. (4.19). Finally, an inverse problem is solved to find the propagation solution $u(\xi,\tau)$ from the scattering data. In general, this involves solving a set of linear integral equations, which reduce to a set of algebraic equations for soliton propagation. The inverse scattering method is summarized in the figure below:
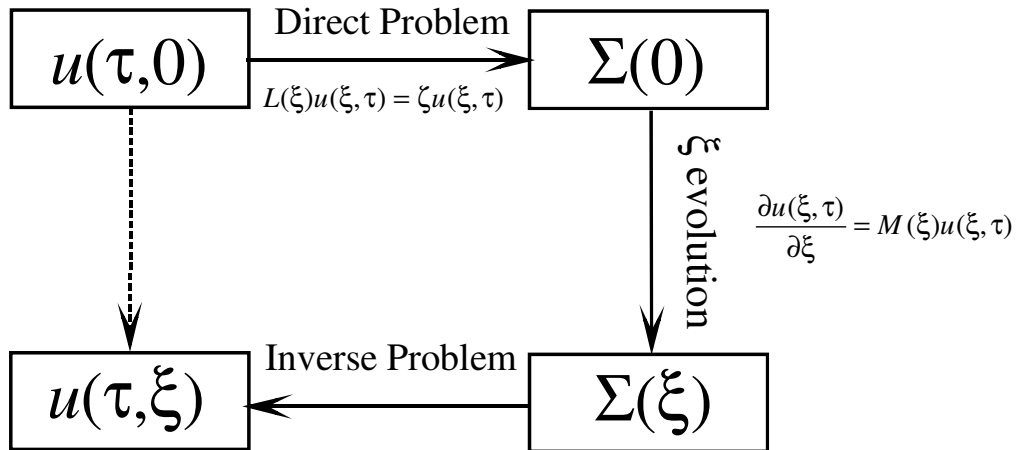

Figure 4.3   Schematic of the inverse scattering method. In the inverse scattering method, the scattering potential Σ serves as a conduit in order to solve for the direct field propagation from $u(t,0)$ to $u(t,\xi)$. First, the initial condition $u(t,0)$ is used with Eq. (4.18) to determine the scattering potential $\Sigma(0)$. Then, Eq. (4.19) is used to determine the ξ propagation of the scattering potential. Finally, the solution $u(t,\xi)$ is found by solving the inverse problem involving the scattering potential $\Sigma(\xi)$.

4.11.2 The Total Field Formulation in the Frequency Domain

Different interactions that occur during the course of nonlinear pulse propagation can generate multiple pulses at different frequencies. However, one electric field $E(z,t)$ should be used to describe these multiple pulse since they all have the same origin from the initial pulse $E(z=0,t)$. Dealing with these multiple pulses may be easier in the frequency domain. Plus, it has been suggested that it is more rigorous to describe both dispersion and nonlinearity in the frequency domain, thus writing the NLSE in terms of z derivatives and multiplication of $i\omega$. The frequency domain representation of the dispersion operator in the SSFM was made out of numerical convenience, making the temporal differential operator in a spectral multiplicative operator. In the total field formulation, both the effect of dispersion and nonlinearity are treated as frequency domain quantities with multiple pulse contained in one field:

$$\frac{\partial E(z,\omega)}{\partial z} = -\frac{\alpha}{2}E(z,\omega) - i\left(\sum_n \frac{\omega^n}{n!}\beta_n\right)E(z,\omega) - i\gamma\left(1+\frac{\omega}{\omega_0}\right)\mathcal{F}\left\{|E(z,t)|^2\,E(z,t)\right\}$$
$$- i\gamma\left(1+\frac{\omega}{\omega_0}\right)\frac{P_0 G_R \omega_0}{c\pi a_0^2}\mathcal{F}\left\{E(z,t)\mathcal{F}^{-1}\left\{S_R\mathcal{F}\left\{|E(z,t)|^2\right\}\right\}\right\}$$

(4.22)

where $S_R(\omega)$ is the complex Raman susceptibility and G_R is the Raman gain coefficient factor.

The advantages of the total field formulation are:
1) The time derivatives $\partial/\partial t$ are replaced by multiplication of $i\omega$.
2) Chromatic dispersion easier to handle in the frequency domain
3) The experimental Raman gain curve, hence the Raman susceptibility is determined by

spectral measurements. Thus a frequency domain representation of SRS may be more accurate.

4) The effect of dispersion and nonlinearity are not handled independently.

Although the total field formulation may be more accurate than the SSFM, a vector computer processor is needed in order to solve Eq. (4.22). Consider the example of soliton propagation through 80 km. The field was sampled by 512 points with Eq. (4.22) solved by numerical integration using a fourth order Runga-Kutta-Felhberg [86] routine per each iteration. A total of 16600 integration steps were necessary for the solution using a vector processor.